Ultrasound in Med. & Biol., Vol. 34, No. 4, pp. 685–688, 2008

0301-5629/08/$–see front matter

ELSEVIER

doi:10.1016/j.ultrasmedbio.2007.10.001

● *Technical Note*

NONSPHERICAL VIBRATIONS OF MICROBUBBLES IN CONTACT WITH A WALL—A PILOT STUDY AT LOW MECHANICAL INDEX

H. J. Vos,* B. Dollet,† J. G. Bosch,* M. Versluis,† and N. de Jong*†‡

*Biomedical Engineering, Thorax Center, Erasmus MC, Rotterdam; †Physics of Fluids, University of Twente, Enschede; and ‡Interuniversity Cardiology Institute of the Netherlands, Utrecht, The Netherlands

(*Received* 25 *June* 2007, *revised* 17 *September* 2007, *in final form* 8 *October* 2007)

Abstract—Radially oscillating microbubbles can deform when in contact with a wall. These nonspherical shapes have a preferential orientation perpendicular to the wall. Conventional microscope setups for microbubble studies have their optical axis perpendicular to the wall (top view); consequently they have a limited view of the deformation of the bubble. We developed a method to image the bubble in a side view by integrating a mirror in the microscope setup. The image was recorded at 14.5 million frames per second by a high-speed camera. When insonified by a 1-MHz, 140-kPa ultrasound pulse, a 9-μm diameter coated bubble appeared spherical in the top view, but strongly nonspherical in the side view. Its shape was alternatively oblate and prolate, with maximum second order spherical harmonic amplitude equal to the radius. (E-mail: H.J.Vos@ErasmusMC.nl)

Key Words: **Ultrasound contrast agent, Bubble wall interaction, Asymmetric oscillation, Orthogonal view imaging.**

INTRODUCTION

Ultrasound contrast agents (UCAs) consist of micron-sized gaseous bubbles, stabilized by a thin coating of phospholipids or denatured albumin. They enhance the echoes from the blood circulation system in the body, facilitating quantification of physiological parameters such as the cardiac output, myocardial perfusion and vasculature of liver carcinoma (Feinstein 2004). More recently, UCA bubbles have been adopted to perform more sophisticated tasks such as specific targeting of bubbles to pathologic tissue, so-called *molecular imaging* (Lindner 2004), and enhancing drug uptake of cells (van Wamel 2006). The physical mechanisms underlying these emerging applications are now the subject of many detailed studies of bubble–wall interactions.

Over the past 15 years, multiple studies have addressed the acoustic response of UCAs. In early years, agents were characterized by the acoustical scattering and attenuation properties of a population of bubbles (de Jong 1992, Hoff 2000). From that moment, advances in experimental technology gradually provided more insight into individual bubble dynamics. Optical systems were developed that fully captured the bubble's behavior. One method exploited laser-light scattering (Guan 2004), which gives a relative value of the instantaneous 1-D size. In 1999, bubble dynamics were resolved in a 1-D streak image using a microscope and camera setup (Morgan 2000). In addition, the camera used by them (Imacon 468, DRS Hadland Inc., Cupertino, CA) could also store seven 2-D frames at high frame rate, facilitating the interpretation of the streak images. Higher frame numbers were available in the Ultranac system (Imacon, 24 2-D frames) (Kuribayashi 1999), and in the Brandaris 128 camera system, which is able to record 128 frames at rates up to 25 million frames per second (Mfps) (Chin 2003). Following this historic line, a setup that is able to image the bubble in three dimensions is believed to provide even more insight into the dynamics of a vibrating bubble.

A typical microbubble setup with a microscope includes an optically and acoustically transparent wall, to which bubbles float up by buoyancy; this allows for precise focusing of the optical equipment. The bubbles are typically imaged by an upright microscope, in which case the optical axis is perpendicular to the wall (top view). At low mechanical index (MI) insonation of <0.04, bubbles were observed to remain spherical during their vibration (van der Meer 2007). At higher pres-

Address correspondence to: H. J. Vos, Room Ee2302 Biomedical Engineering, Erasmus MC, PO Box 2040, 3000CA Rotterdam, The Netherlands. E-mail: H.J.Vos@ErasmusMC.nl

sures and long bursts, parametric instabilities lead to nonspherical surface modes, a range of ultrasound conditions that we do not address in this paper. From literature, it is known that vibrating bubbles close to or in contact with a wall can show nonspherical shapes oriented perpendicularly to the wall (Blake 1986; Fong 2006; Prentice 2005; Zhao 2005). In numerical simulation studies by Fong et al. (2006), this effect was already significant after excitation of a bubble with a 1.5 cycle, 80-kPa ultrasound pulse at its resonance frequency. Their model excluded any viscous and thermal damping and assumed a free gas–liquid surface of the bubble. In studies of UCA bubbles, the nonspherical oscillations were thought to be less significant because the coating of UCA microbubbles was expected to damp potential nonspherical oscillations. However, the commonly used vertical microscope setups do not allow for imaging such nonspherical phenomena that are expected to occur in line with the optical axis.

Thus, our aims here were two-fold. The first was to develop a method to quasi-instantaneously project the bubble vibration in two orthogonal planes, as an improvement to the 2-D setups used in the past. The second was to estimate the amplitude of potential nonspherical oscillations of a UCA bubble in contact with a rigid wall. The method and first results are presented here.

MATERIALS AND METHODS

The experimental setup (Fig. 1) consisted of a mirror, a microscope and the high-speed Brandaris 128 camera (Chin 2003). Highly diluted Definity agent (Bristol Myers Squibb MI, N. Billerica, MA, USA) was inserted in a cellulose tube (Cuprophan, Akzo Nobel Faser AG, Germany), which has an inner diameter of 160 μm and wall thickness of 20 μm, and which was submersed in a water tank.

Buoyancy forces the bubbles in the agent to float to the top. There they were imaged along two perpendicular optical axes and denoted “top view” and “side view,” respectively. In top view, a single bubble is imaged from above, which is the conventional optical detection mode. In the side view mode, the bubble is observed through a mirror positioned at an angle of 45° to the optical axis of the microscope. The viewing mode is selected by adjusting the position of the microscope with respect to the mirror. The distance between the bubble in the tube and the mirror surface was 0.50 mm.

Ultrasound pulses were generated by a 1-MHz broadband focused transducer (V302-SU 3″, Panametrics-NDT, Waltham, MA, USA), which was driven by a high-power RF linear amplifier (ENI A-500, Rochester, UK). The ultrasound pulse contained six cycles at 1 MHz with a cosine-tapered window. The pressure in the focus of the transducer, 140 kPa in the experiment reported here, was measured with a calibrated hydrophone in a separate setup.

RESULTS

A bubble with a diameter of 9 μm, which is close to the expected resonant size at 1 MHz for a similar type of microbubble (van der Meer 2007), was studied in these experiments. The oscillation dynamics were recorded in top view mode. Next, the dynamics of the very same bubble were recorded in side view mode. Both recordings contain 128 frames at a rate of 14.5 Mfps, and 16 frames of each recording are selected for Fig. 2. The sequence in Fig. 2 starts at maximum expansion of the bubble and covers two cycles of ultrasound insonation.

In top view (top panel of Fig. 2), the bubble shows a circular shape throughout, without deformation. When viewed from the side (bottom panel), a strikingly different behavior is observed. In frame 3, the bubble shape is strongly prolate (defined by having two short axes and one long axis). In frames 4–6, the original bubble even seems to split momentarily. Between frames 9 and 10, the bubble wall velocity in the sequence is one order higher (10 μm/0.14 μs $\sim$ 70 m/s) than the typical wall

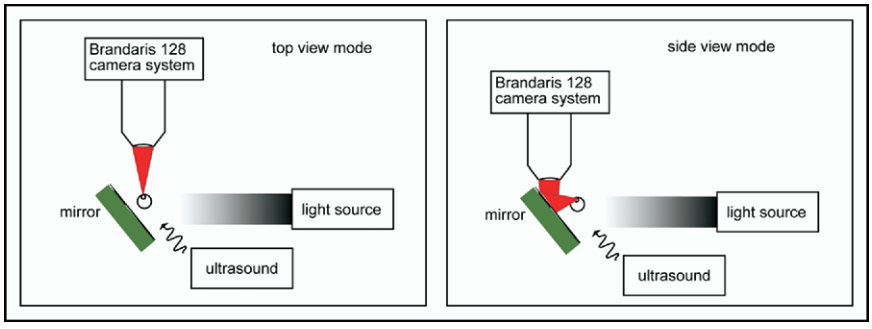

Fig. 1. Experimental setup. The bubble is imaged inside the capillary tube, and the imaging mode (top view or side view) is selected only by the position of the microscope.

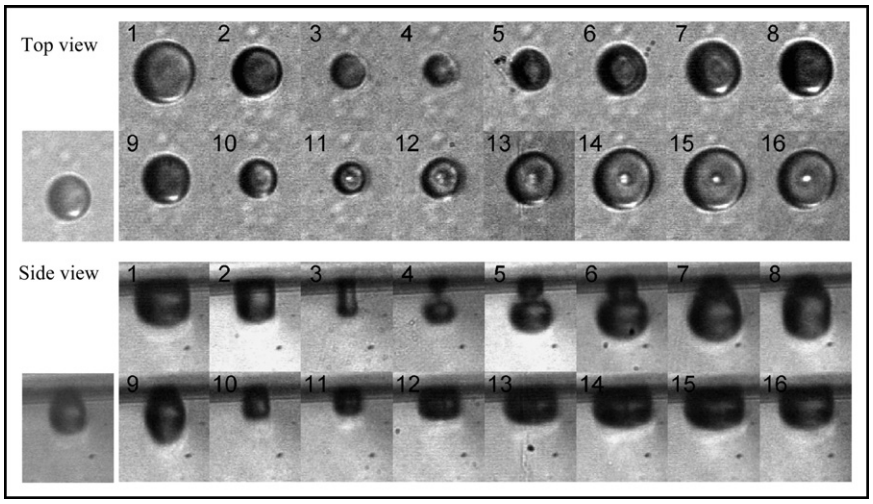

Fig. 2. Optical images of the bubble during two cycles of the ultrasound pulse. Top panel shows top view images at an interframe time of 138 ns. Bottom panel shows the same segment of bubble oscillations in side view, recorded 2 min later. The bubble wall appears as a grey region on the top. Resting diameter of the bubble (left) was 9 μm.

velocity during oscillation. Starting in frame 12, the bubble shows a strongly oblate shape (*i.e.*, two long orthogonal axes and one short), until the shape of frame 16 resembles the one in frame 1.

The circumferential edge of the bubble was tracked using a special implementation of a minimum cost algorithm in all frames (Bosch 1995). In this implementation, the contour in the previous frame was used as an estimate in the next frame and in two iterations the final shape was detected. The algorithm does not assume a spherical or convex shape. Decomposition of the circumferential edge into spherical harmonic amplitudes involved two steps. First, the contour was mapped onto polar coordinates (R,θ) having its origin in the center of gravity. Second, the amplitudes A_n for $n = 0$ and $n = 2$ were calculated from $R(\theta)$ using the Legendre polynomials,

$$A_n = (0.5 + n)\int_0^{\pi} R(\theta)P_n(\cos\theta)\sin(\theta)d\theta, \qquad (1)$$

where P_n represents the Legendre polynomial of order n. These steps were repeated for all frames. In the present configuration, a positive value of A_2 denotes a prolate shape.

Figure 3 shows the amplitudes of the modes as observed in top view and side view as a function of time. The top panels show the radial mode excursion, and the

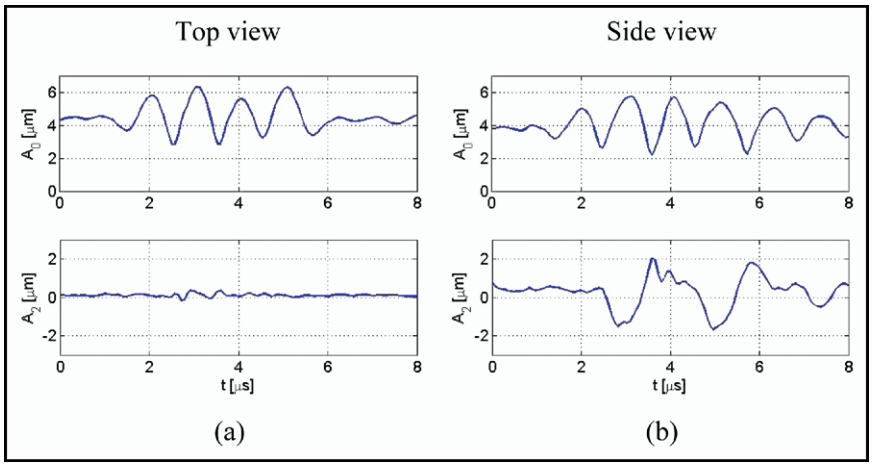

Fig. 3. Amplitudes of the radial oscillation A_0 (top panel) and second-order surface modes A_2 (bottom panel) as a function of time, when (a) was imaged from the top and (b) was imaged from the side.

bottom panels show the amplitudes of the second-order shape mode. In the top view mode, the maximum radial excursion shows a 1.8 μm amplitude (40% of the initial radius) and second-order surface modes show negligible amplitude.

The side view analysis shows a radial oscillation having an initial increase of the amplitude (0–2.5 μs), a steady state oscillation (2.5–4.5 μs) and decaying amplitude (4.5–8.5 μs). The second-order shape oscillation shows significant amplitude, up to 2 μm, which is equal to the instant radius at that instant of time. It also displays a clear subharmonic behavior. Note that the bubble size was reduced by 10% in the 2-min interval between the two recordings.

DISCUSSION

The side view setup has sufficient spatial and temporal resolution to resolve the oscillatory shapes of a microbubble in contact with a rigid wall, at low MI (0.14). The observed nonspherical shapes are not visible in the conventional imaging (top view) mode, because the deformation has an orientation perpendicular to the wall; a projection in top view of such a deformed bubble is circular. Moreover, the bubble volume cannot be quantified from the projected area observed in top view because the oblate shape appears larger than the prolate shape, even though the volume of the bubble is conserved in the rarefaction phases of the ultrasound pulse. As a consequence, in top view, the alternating oblate and prolate shapes appear as an additional subharmonic oscillation, *i.e.*, an oscillation with a frequency equal to half the excitation frequency. This could explain the results found by Zhao et al. (2005) regarding their observed subharmonic vibrations.

In this experiment, the amplitude of the second-order nonspherical vibration reached values about equal to the instantaneous radius, leading to a transient breakup of the bubble. Such finding is in line with the findings of Zhao et al. (2005) who also found strong prolate and oblate shapes for UCA bubbles excited at an MI of 0.2. Prentice et al. (2005) used an optical tweezer to position a microbubble close to a wall and insonified it at higher MI (0.7) than we used here. They showed that jets can occur, which are deformations in an extreme sense. On the other hand, Garbin et al. (2007) have shown that for low MI insonation, no significant deformations occur when bubbles interact with a wall or neighboring bubbles.

As mentioned in the Results section, the bubble slightly reduced its size in the second sequence. Such a deflation may have an effect on the shell structure and, consequently, on the overall bubble-dynamics. The deflation of the bubble should be considered when modeling the bubble behavior in three dimensions and therefore our setup is now being adapted to allow for a simultaneous imaging of the bubble in both a top view and a side view.

Further studies using the proposed side-view method could assist in establishing more quantitative understanding of the observed bubble-wall interaction, and might separate a range of conditions for which the nonspherical phenomena are significant from a range where they are not. The method can also be used to study the interactions between bubbles and biological tissue, providing detailed knowledge on mechanisms related to molecular imaging and drug delivery applications.

REFERENCES

Blake JR, Taib BB, Doherty G. Transient cavities near boundaries. Part 1. Rigid boundary. J Fluid Mech 1986;170:479–497.

Bosch JG, Savalle LH, van Burken G, Reiber JHC. Evaluation of a semiautomatic contour detection approach in sequences of short-axis two-dimensional echocardiographic images. J Am Soc Echocardiogr 1995;8:810–821.

Chin CT, Lancée CT, Borsboom JMG, Mastik F, Frijlink ME, de Jong N, Versluis M, Lohse D. Brandaris 128: A 25 million frames per second digital camera with 128 highly sensitive frames. Rev Sci Instr 2003;74:5026–5034.

de Jong N, Hoff L, Skotland T, Bom N. Absorption and scatter of encapsulated gas filled microspheres: Theoretical considerations and some measurements. Ultrasonics 1992;30:95–103.

Feinstein SB. The powerful microbubble: From bench to bedside, from intravascular indicator to therapeutic delivery system, and beyond. Am J Physiol Heart Circ Physiol 2004;287:H450–457.

Fong SW, Klaseboer E, Turangan CK, Khoo BC, Hung KC. Numerical Analysis of a gas bubble near bio-materials in an ultrasound field. Ultrasound Med Biol 2006;32:925–942.

Garbin V, Cojoc D, Ferrari E, Fabrizio ED, Overvelde MLJ, van der Meer SM, de Jong N, Lohse D, Versluis M. Changes in microbubble dynamics near a boundary revealed by combined optical micromanipulation and high-speed imaging. Appl Phys Lett 2007; 90:ref. 114103.

Guan J, Matula TJ. Using light scattering to measure the response of individual ultrasound contrast microbubbles subjected to pulsed ultrasound *in vitro*. J Acoust Soc Am 2004;116:2832–2842.

Hoff L, Sontum PC, Hovem JM. Oscillations of polymeric microbubbles: Effect of the encapsulating shell. J Acoust Soc Am 2000; 107:2272–2280.

Kuribayashi K, Kudo N, Natori M, Yamamoto K. A high-magnification and high-speed system for the observation of microbubbles under ultrasound exposure. IEEE Ultrasonics Symp, Lake Tahoe, Nevada, 1999.

Lindner JR. Microbubbles in medical imaging: current applications and future directions. Nat Rev Drug Disc 2004;3:527–532.

Morgan KE, Allen JS, Dayton PA, Chomas JE, Klibanov AL, Ferrara KW. Experimental and theoretical evaluation of microbubble behavior: Effect of transmitted phase and bubble size. IEEE Trans Ultrason Ferroelectr Freq Control 2000;47:1494–1509.

Prentice P, Cuschieri A, Dholakia K, Prausnitz M, Campbell P. Membrane disruption by optically controlled microbubble cavitation. Nat Phys 2005;1:107–110.

van der Meer SM, Dollet B, Voormolen MM, Chin CT, Bouakaz A, de Jong N, Versluis M, Lohse D. Microbubble spectroscopy of ultrasound contrast agents. J Acoust Soc Am 2007;121:648–656.

van Wamel A, Kooiman K, Harteveld M, Emmer M, Ten Cate FJ, Versluis M, de Jong N. Vibrating microbubbles poking individual cells: Drug transfer into cells via sonoporation. J Control Release 2006;112:149–155.

Zhao S, Ferrara KW, Dayton PA. Asymmetric oscillation of adherent targeted ultrasound contrast agents. Appl Phys Lett 2005;87:ref. 134103.